Radiolysis effect on Eu(III)-superplasticiser interactions in artificial cement and squeezed cement pore waters

Solène Legand, Nathalie Macé, Benoist Muzeau, Philippe Le Tutour, Sandrine Therias, Pascal Reiller

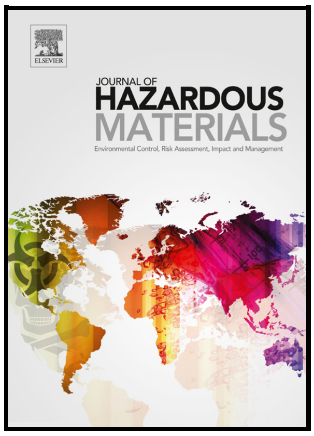

Radiolysis effect on Eu(III)-superplasticiser interactions in artificial cement and squeezed cement pore waters.

Solène Legand, Nathalie Macé, Benoist Muzeau, Philippe Le Tutour, Sandrine Therias, Pascal E. Reiller

PII: S0304-3894(22)02063-5

DOI: https://doi.org/10.1016/j.jhazmat.2022.130269

Reference: HAZMAT130269

To appear in: *Journal of Hazardous Materials*

Received date: 20 July 2022
Revised date: 6 October 2022
Accepted date: 24 October 2022

Please cite this article as: Solène Legand, Nathalie Macé, Benoist Muzeau, Philippe Le Tutour, Sandrine Therias and Pascal E. Reiller, Radiolysis effect on Eu(III)-superplasticiser interactions in artificial cement and squeezed cement pore waters., *Journal of Hazardous Materials,* (2022) doi:https://doi.org/10.1016/j.jhazmat.2022.130269

Radiolysis effect on Eu(III)-superplasticiser interactions in artificial cement and squeezed cement pore waters.

Solène Legand,[a,*] Nathalie Macé,[a] Benoist Muzeau,[a] Philippe Le Tutour,[a] Sandrine Therias,[b] Pascal E. Reiller[c]

[a] *Université Paris-Saclay, CEA, Service d'Études du Comportement des Radionucléides (SECR), F-91191 Gif-sur-Yvette, France.*

[b] *Université Clermont Auvergne-CNRS, ICCF F-63000 Clermont–Ferrand, France.*

[c] *Université Paris-Saclay, CEA, Service d'Études Analytiques et de Réactivité des Surfaces (SEARS), F-91191 Gif-sur-Yvette, France.*

[*] *corresponding author: solene.legand@cea.fr*

KEYWORDS: Superplasticizers, radiolysis, hydrolysis, degradation, speciation, solubility, complexation, europium

Abstract

In the framework of the French deep geological repository for radioactive waste, cement-based materials are envisaged to immobilize radionuclides and/or provide protection from radiation to the environment. Superplasticisers (SPs) are added to these materials to increase their workability. SPs will undergo degradation by coupled radiolytic and hydrolytic effects in the pore solution leading to the formation of potentially complexing degradation products. The objective was to study the potential effect of radiolyzed superplasticizers contained in cement-based materials on radionuclide uptake. The Eu speciation and solubility with organic ligands resulting from the degradation of SPs were studied for the two solutions and the results were compared. Two different SPs were selected, a polycarboxylate ether and a polynapthalene sulfonate. Two different protocols were followed: direct irradiation of the solution containing the superplasticizer, and irradiation of the compacted cement sample followed by extraction of the pore water. Solubility enhancements observed in artificial

cement waters are not representative of real cement pore water interactions, in agreement with other studies. Finally, the effects of alkaline hydrolysis and radiolysis of SPs on Eu solubility in pore water are limited.

1 Introduction

In the French nuclear waste management context, the intermediate-level long-lived waste should be stabilized in mortar or concrete matrix. The cemented waste forms are used to provide protection from radiation to man and the environment during the repository and/or immobilize radionuclides (RNs) in the context of disposal. In such cement-based materials, superplasticisers (SPs) are used as admixtures to increase the workability of the early-aged cement-water-aggregate mixture. In a deep geological repository scenario, SPs should undergo degradation by radiolysis and hydrolysis in the pore solution of cement-based materials (Chantreux et al., 2021), leading to the formation of potentially complexing degradation products. Determining the impact of SP degradation products (DPs) on the complexation with radionuclide and so RNs migration through cementitious materials is important when assessing the disposal concept (Andra, 2005).

There are different families of SPs, as described by Flatt and Schober (2012): lignosulfonates; polynaphthalene sulfonates (PNS) and polymelamine sulfonates; monochain polyethylene glycol with a phosphonate group; polycarboxylate or polycarboxylate ether (PCE). This list is not exhaustive and keeps on evolving. New formulations of SPs are emerging such as polyarylether (Chernyshev et al., 2018). Amongst SPs, the effect of alkaline hydrolysis on PCE (Baston et al., 2019; Felekoğlu and Sarıkahya, 2008; García, 2018; Guérandel et al., 2011; NDA, 2015; Palacios and Puertas, 2004) and PNS (Palacios and Puertas, 2004; Yilmaz et al., 1993), has been studied more than the radiolysis. For PCE, these studies showed the side chains of polyether detach from the main carbon chain. These cuts are due to the cleavages of the ester

groups (Palacios and Puertas, 2004). The hydrolysis studies of these SPs in solution, or as adjuvants in cementitious materials, have shown significant degradation at pH above 13. The radiolysis studies were carried out mainly under γ-radiation for PCE (Baston et al., 2019; García, 2018) and PNS (Lezane, 1994). These studies suggested a complex and non-predictable degradation (Baston et al., 2019). The phenomena observed after irradiation of an SP are different in its solid form, in solution, or added to the cementitious material. This is mainly due to conditions that strongly vary the amount of SPs, pH, and oxygen content. The primary radicals react with oxygen to form peroxyl radicals that initiate chain reactions of oxidation and the formation of hydroperoxides. The reactions of radicals with each other lead to the formation of oxidation products — e.g. ketones, aldehydes, acids, alcohols, esters (Von Sonntag, 2003). The degradation is also dependent on the nature of the SP and the received dose (Baston et al., 2019; García, 2018). In alkaline solution, it seems that the SP under radiation: (i) undergoes limited damage at very low doses (< 10 kGy) (Baston et al., 2019); (ii) depolymerizes at intermediate doses (from 10 to 200 kGy) (Baston et al., 2019); and (iii) crosslinks at higher doses (> 200 kGy) (García, 2018). The side chains of polyethylene glycol PEG seem brittle (Baston et al., 2019; García, 2018), whereas the aromatic structure of PNS seems more resistant (Lezane, 1994). Although some studies showed an evolution of PCE, no exhaustive inventory of the degradation products formed has been proposed by Baston et al. (2019).

As it has been shown otherwise for radiolysis DPs of polymers (Fromentin et al., 2020; Reiller et al., 2017), the interactions between europium(III) and organic ligands of SP type in a cement medium have been carried out in some studies. Fröhlich et al. (2019, 2017) and Chernyshev et al. (2021) have observed the interaction between europium(III) and a PCE. Greenfield et al. (1998) and Clacher et al. (2013) have shown that if an SP is introduced into solution at pH 12 and 12.5, respectively, it will increase the solubility of Am/Eu, even when

the SP is present in very low concentration (< 0.1 wt% SP in solution). However, this increase in solubility was not observed when solubility studies were carried out in the presence of water brought into contact with admixed cementitious materials or interstitial solution from an admixed cementitious material (Clacher et al., 2013; Greenfield et al., 1998; Kitamura et al., 2013; Lezane, 1994). These observations have shown that not all organic molecules from SPs were released in pore solution. The quantity and type of molecules in solution were different : a small quantity of molecules is released in concrete-equilibrated water (Greenfield et al., 1998) and the size of molecules is different from SPs (Clacher et al., 2013). This hypothesis remains to be confirmed. Only the study of Kitamura et al. (2013) from an admixed cementitious material; no significant increase of the americium solubility has been observed. The effects obtained by adding an SP in solution did not seem representative of those observed in interstitial solution. So, it is difficult to predict the solubility of RNs in pore solution of admixed cementitious materials with water brought into contact with admixed cementitious materials. To the best of our knowledge, no Am/Eu solubility study has shown results in pore solution from irradiated admixed cementitious materials, or even in irradiated cementitious solution initially containing PCE or PNS to understand the impact of radiolysis on the SP in interstitial or cementitious solution.

In this work, two different SPs have been studied from the two families PCE and PNS, after γ-irradiation at different doses between 0 and 250 kGy, in the presence of Eu(III) taken as chemical analogue of trivalent actinides. The study tries to understand how representative are artificial cement water compared to pore solution. The main objectives of this work are: (i) to better understand the behaviour of SPs subjected to the coupled effect of radiolysis and alkaline hydrolysis; (ii) to quantify the interactions between Eu(III) and organic ligands resulting from the degradation of SPs; and (iii) to compare the effect of radiolyzed SPs in artificial cement water and from irradiated admixed cementitious materials.

2 Materials and methods

2.1 Materials

Commercial SP solutions were used without any further purification. The commercial SPs were MasterGlenium 201 and Sikafluid for PCE and PNS, respectively. The density and dry extract were (1.05 ± 0.02) g cm^{-3}, (19.9 ± 2.0) wt% for PCE and (1.15 ± 0.03) g cm^{-3}, (32.5 ± 1.6) wt% for PNS. In the following, the commercial SP solutions will be named PCE and PNS, not to be confused with the PCE and PNS pure polymer, respectively.

Two types of alkaline solutions have been used: (i) irradiated SP alkaline solutions; and (ii) pore solutions obtained by pressing irradiated SP-grout. Irradiated SP alkaline solutions initially contained 1 and 2 wt% of PCE and PNS in solution, respectively. Pore solutions have been selected as reference to a system of SP-based compact cement. SP alkaline solutions were prepared by adding either PCE or PNS to alkaline solutions under inert conditions (under Ar and O_2 < 1 %). The alkaline solution contained 0.15 mol L^{-1} NaOH (AnalaR NORMAPUR, VWR), 0.12 mol L^{-1} KOH (EMSURE ACS, Merck), and 10 g L^{-1} of a crushed SP-admixed cement-based material. The solutions were filtered (polyether sulfone syringe filter 0.2 µm sterile diameter 25 mm, Thermofisher). The SP alkaline solutions had a resulting pH value of 13.3 ± 0.1 (cf. § 2.2.1 for standardization method), which is in agreement with a theoretical calculation using PHREEQC version 3.6.2. 15100 (Parkhurst and Appelo, 1999) with the PSI/NAGRA database (Thoenen et al., 2014). SP-grouts were prepared by mixing cement (CEM I 52.5 N - SR 5 CE PM-CP2 NF HTS Le Teil), filler (Sibelco E600), SP, and water (Ultrapure Milli-Q water Millipore, 18.2 MΩ.cm at 25°C, COT < 5ppb_C) with a water/cement ratio of 1.5, a filler/cement ratio of 2.0, an SP/water ratio of 1.3 and 2.7 wt% for PCE and PNS, respectively. The grouts were cured in closed reactors for 28 days at a relative humidity of 95% before further use. Pore solutions were obtained after cure and irradiation. A high-

pressure device designed by Cyr et al. (2008; 2007) was used. Cyr et al. (2008) highlighted the impact of extraction protocol on efficiency of extraction and repeatability of measurement. Nevertheless, the authors concluded that for a pressure between 500 and 1000 MPa, the chemical composition (Ca, Na, K, and Si) of the pore solution is not significantly different. The grouts was pressed from 0 to 200 MPa in increments of 10 MPa, and from 200 to 700 MPa in increments of 50 MPa with a step of 1 min (ENERPAC, 2000 kN hydraulic press). The grout of 118 cm^3 (205 g) allowed us to obtain around 9 mL of pore water. The pore solution's pH value was measured at (12.9 ± 0.1). The SP alkaline solution and SP-grout were degraded by γ-radiolysis, which was performed at the Poseidon irradiator (Laboratory for radiation applications, LABRA, CEA Saclay, France). The irradiator was equipped with ^{60}Co sources. Dosimetry was performed using a UNIDOS PTW dosimeter equipped with a calibration chamber. Dosimetry was performed just before irradiation by placing the ionization chamber of the dosimeter at the same place as the samples. The dosimetry revealed an attenuated dose of 6% between the dose measured in the air and that at the heart of the solution, and 15% between the dose deposited in the air and that at the heart of a block. The selected dose rate of 1 kGy h^{-1} corresponds to highly irradiating waste; irradiations can be carried out in reasonable time. Exact irradiation doses in the heart of samples (alkaline solution or grout) were determined 23.5, 47.1, 94.1, and 260.5 kGy. In the following, only the targeted doses, i.e., 25, 50, 100, and 250 kGy will be referred to ease the reading. The applied doses are representative of the dose received over 100 years for the least irradiating waste; they are interesting in first approach to observe the degradation over a short time period.

The SP alkaline solutions and pore solutions were filtered through Thermo Scientific Nalgene syringe filters equipped with a PES membrane (0.2 µm size pore × 25 mm i.d.) prior to characterizations or used in solubility/speciation experiments.

2.2 Methods

The SP degradation products, pH of the solutions, and cation concentrations (Ca, K, and Na), were measured by pH measurements, total organic carbon content (TOC), ion chromatography (IC), silicate quantification, and size exclusion chromatography (SEC). The interaction of Eu(III) with SP degradation products was investigated by the measurement of Eu solubility using spikes of ^{152}Eu ($T_{1/2}$ =13.522 yr, 88.8% γ-emitter, 121.8 keV), and the speciation of Eu-ligand by time-resolved laser-induced fluorescence spectroscopy (TRLFS).

2.2.1 *pH measurements*

The pH measurements were made using a PHM250 pHmeter (Radiometer Analytical) with a temperature probe and a combined pH micro-electrode (ref 6.0234.100, Metrohm). The reference electrolyte was a 3 mol L^{-1} KCl solution. Calibration was carried out using 3 Certipur buffer solutions (Merck) with theoretical pH values at 22°C of 7.01 (potassium dihydrogen phosphate and di-sodium hydrogen phosphate), 9.20 (boric acid, KCl and NaOH), and 12.09 (di-sodium hydrogen phosphate and sodium hydroxide). An alkaline solution (0.13 mol L^{-1} NaOH and 0.12 mol L^{-1} KOH) whose pH was estimated at 13.2 by PHREEQC calculations — using PSI/NAGRA database (Thoenen et al., 2014) — was prepared to check the linearity of the calibration above pH = 12. The pH measurements were made with an uncertainty calculated at 2σ or 0.1 pH unit.

2.2.2 *Total organic carbon (TOC)*

The total organic carbon (TOC) content was determined indirectly based onto the total inorganic carbon (TIC) and total carbon (TC) measurements. The TIC and TC measurements were performed using a VARIOTOC cube analyser (Elementar). The TIC was measured by acidifying the sample with a diluted H_3PO_4 solution prepared from a concentrated commercial

one (85%, Merck). The TC was obtained by a Pt-catalytic combustion at 850°C of the liquid samples. After TIC and TC reactions, the produced-CO_2 gas was measured by IR. The TOC concentration in the sample was then obtained by the difference between the TC and the TIC concentrations. The calibration was done using standard solutions prepared by mixing with Milli-Q-water potassium hydrogen phthalate ($K_2H_4O_4C_8$, Elementar S35.00-0151) to reach 0.08 to 2.08 10^{-3} mol L^{-1} of carbon (mol_C L^{-1}) in TOC and anhydrous sodium carbonate (Na_2CO_3, Elementar S35.00-0152) to reach 0.08 to 2.08 10^{-3} mol_C L^{-1} in TOC in TIC. The injected volume was 0.1 mL and each sample was analysed 3 times. A blank consisted in Milli-Q-water was inserted between each sample to measure the background in TIC and TC.

2.2.3 *Ion chromatography (IC)*

Following the standard procedures in the laboratory, two different IC set-ups were used. Acetate (CH_3COO^-), SO_4^{2-} and SO_3^{2-} anions were detected by conductivity on an Integrion Ion Chromatography System (Thermofisher, Dionex) controlled by the Chromeleon software. The guard column employed was a Hydroxide-Selective Anion-Exchange Dionex IonPac AG15 RFIC 2 mm i.d. × 50 mm L and the column was an AS15 2 mm i.d. × 250 mm L, both maintained at 30°C. The elution was obtained by isocratic method at 38 mmol L^{-1} of KOH for 40 min. The flow rate was 0.3 mL min^{-1} and the sample injection volume was fixed at 10 µL. The calibration was performed on standard solutions prepared by diluting in Milli-Q-water a standard acetate solution at 1000 mg L^{-1} (Sigma-Aldrich, TraceCERT 51791), a standard sulfate solution at 1000 mg L^{-1} (Fisher Chemical J/4564/05) and a powder of anhydrous Na_2SO_3 (Sigma Aldrich 31454). Standard solutions ranged from 0.5 to 50 mg L^{-1}.

Cl^-, Na^+, K^+, and Ca^{2+} species were detected on an 850 Professional Ion Chromatography System (Metrohm) by conductivity and controlled by the MagIC Net software. The sample injection volume was fixed at 10 µL. The Cl^- elution was obtained on a Metrosep A supp 7

column (4 mm i.d. × 150 mm L) by isocratic method at 3.6 mmol L^{-1} of $NaCO_3$ with a flow rate of 0.8 mL min^{-1} for 22 min. The cations elution (Na^+, K^+, Ca^{2+}) was obtained on a Metrosep C4 column (4 mm i.d. × 150 mm L) by isocratic method at 3 mmol L^{-1} of HNO_3 with a flow rate of 0.7 mL min^{-1} for 24 min. The calibration was performed on standard solutions at 1 000 µg mL^{-1} (Chem-Lab) prepared by diluting in Milli-Q-water or HNO_3 for anions and cations respectively. Standard solutions ranged from 0.05 to 5 mmol L^{-1} for Na^+, K^+, and Cl^-, and 0.02 to 0.5 mmol L^{-1} for Ca^{2+}.

For the two systems, standard solutions were injected in triplicates and blanks of Milli-Q-water were injected before each sample. Samples diluted in Milli-Q-water were also injected in triplicate to estimate standard deviations (σ). The uncertainty was estimated at 2σ.

2.2.4 *Silicate quantification*

Silicate quantification was based on the formation of molybdenum blue complex (Zini et al., 1985), using the colorimetric method (Spectroquant kit, 1.14794.0001, Merck) at 810 nm using a UV-Visible Cary 50 spectrophotometer (Varian). The standards were obtained from dilution of the 1000 mg L^{-1} standard solution to concentrations between 0 and 1.5 mg L^{-1} Si (i.e. 0 to 4.2 10^{-5} mol_{Si} L^{-1}). Each sample was analysed 5 times. The measurements were carried out with an uncertainty calculated at 2σ.

2.2.5 *Size exclusion chromatography (SEC)*

The SEC system used was U3000 Chromatography System (Thermofisher, Dionex) controlled by the Chromeleon software. The PCE was detected by ERC refractoMax 520 refractive index detector (RI) and the PNS by Dionex PDA 100 Photodiode Array Detector (UV-visible detector at 290 nm). The guard column employed was a Tosoh TSKgel superAW-L (4.6 mm i.d. × 3.5 cm L) and two columns in series were Tosoh TSKgel superAW4000 (6.0 mm i.d. × 15 cm L

× 6 µm particle size), all maintained at 35°C. The elution was obtained by the isocratic method at 10 mmol L^{-1} of ammonium acetate (Analypur, Fisher Scientific) for 40 min. The flow rate was 0.2 mL min^{-1} and the sample injection volume was fixed at 20 µL. The standard calibration was not applicable to SPs. The supply of reference standards (molar mass distribution close to 1) having a polymeric structure and molar masses close to that of the translated SPs was not possible. The irradiated samples were compared relatively to each other.

2.2.6 *Europium operational solubility measurement*

The Eu(III) operational solubility was measured by oversaturation experiment. The Eu solubility limit in the medium ($S_{max,Eu}$) was estimated at $10^{-(6.1 \pm 0.9)}$ mol L^{-1} at pH 13.3 using the PSI/NAGRA database (Thoenen et al., 2014), considering amorphous $Eu(OH)_3$(am) as solubility limiting phase as in previous studies (Fromentin et al., 2020; Reiller et al., 2017).

$$Eu(OH)_3(am) + 3H^+ \rightleftarrows Eu^{3+} + 3H_2O \qquad \log_{10}K_s = 17.6 \pm 0.8 \tag{1}$$

and the formation of the first three hydroxo complexes — mainly the trihydroxo complex $Eu(OH)_3$(aq).

$$Eu^{3+} + 3H_2O \rightleftarrows Eu(OH)_3(aq) + 3H^+ \qquad \log_{10}{}^*\beta°_3 = -23.7 \pm 0.1 \tag{2}$$

The formation of $Eu(OH)_4^-$ was not considered, as explained elsewhere (Hummel et al., 2002).

The solubility under these conditions is then governed by the product $K_s\,{}^*\beta°_3$.

$$\log_{10} S_{max,Eu} = \log_{10} K_s + \log_{10}{}^*\beta°_3 = -6.1 \pm 0.9 \tag{3}$$

A mixture of $EuCl_3{:}6H_2O$ powder (powder Alfa Aesar, REacton, 99.99%, 11297) and Eu radioactive solution (ELSB45, LEA-Orano) — containing $EuCl_3$ as carrier with $[Eu_{total}] = (5.4 \pm 1.1)\ 10^{-2}$ mol L^{-1} and ^{152}Eu with an activity $A(^{152}Eu) = (5.7 \pm 1.1)\ 10^5$ Bq g^{-1} of solution — is

added to each SP alkaline solution. A total Eu concentration of 10^{-4} mol L^{-1}, including a spike of radioactive ^{152}Eu solution (2 kBq g^{-1}), was reached. Solubility experiments were performed under inert conditions (glove box under argon) to avoid carbonation. After equilibration time from between one hour to 15 days, the solutions were ultra-centrifuged at 20,000 rpm during 1 h (36,400 g, Coulter Optima L-90K, Beckman). Aliquots from the supernatants were analyzed using a γ–counter (Wizard2 2480 automatic gamma counter, Perkin Elmer) to determine the residual amount of the radioactive tracer in solution. The measure of residual amount of the radioactive tracer in solution after different equilibration time allowed knowing that a balance was achieved; this residual amount being unchanged between one hour to 15 days, the balance was achieved and the first measurement obtained at one hour has been then used in this study. At this initial concentration of Eu (10^{-4} mol L^{-1}), the sorption on tube walls was checked by a europium mass balance and was considered negligible.

The experimental detection limit (DL_{exp}) corresponded to the minimal achievable Eu concentration accounting for three parameters. First, the detection limit of the γ–counter was set to 3 times the background value. Second, the counting efficiency for ^{152}Eu — more than 90% in the 0-2000 keV window. Third, the total Eu concentration of the radioactive source, i.e., 5.4 10^{-2} mol L^{-1}. The DL_{exp} value was calculated to be 1.1 10^{-7} mol L^{-1} for the sample volume (12 mL).

2.2.7 *Time-resolved laser-induced fluorescence spectroscopy (TRLFS)*

As in the previous section, $EuCl_3{:}6H_2O$ powder was used as a precursor to reach 10^{-6} mol L^{-1} of Eu(III) in PNS or PCE alkaline solution . This concentration was considered to be lower than the Eu solubility limit in these media — see previous operational determination (Fromentin et al., 2020; Reiller et al., 2017), and limiting solubility phases calculation. The sample was introduced into a fluorescence quartz cell (Hellma QS-111-10-40). The solution was

submitted to excitation by a pulsed (10 Hz) Nd:YAG laser (Surelite, Continuum). The tripled frequency (355 nm) was adjusted to 393.8 nm using an optical parametric oscillator (OPO) (Horizon, Continuum), which corresponds to an excitation wavelength in the $^5L_6 \leftarrow ^7F_0$ transition of Eu(III) (Carnall et al., 1968). The incident laser energy (typically 3-4 mJ) was monitored using a Joule-meter (RJP-734, Laser Probe Inc.,) placed after the sample holder. The luminescence was collected at 90° with respect to the incident beam. Eu(III) is de-excited by emitting two groups of emission bands; the most used comes from the energy transfer from $^5D_1$ to the $^5D_0$ level, and de-excitation to the ^7F_j ground state manifold ($^5D_0 \rightarrow ^7F_j$, j = 0 to 6, τ ca. 110 µs for Eu^{3+}) (Binnemans, 2015; Horrocks and Sudnick, 1979). The most intense lines correspond to transitions $^5D_0 \rightarrow ^7F_1$ (λ ca. 591 nm), $^5D_0 \rightarrow ^7F_2$ (λ ca. 615 nm) and $^5D_0 \rightarrow ^7F_4$ (λ ca. 694 nm). The intensity ratio between the $^5D_0 \rightarrow ^7F_2$ and $^5D_0 \rightarrow ^7F_1$ ($^7F_2/^7F_1$) transitions is commonly used to plot complexometric curves (Dobbs et al., 1989; Fromentin et al., 2020; Fromentin and Reiller, 2018; Reiller et al., 2017). The spectrometer (Acton) converts the light signal into an electrical signal. It is composed of a grating (the 300 lines mm^{-1} was chosen) and a CCD sensor (1024 diodes, Andor) cooled by Peltier effect at -10°C and synchronized with the pump laser pulses (Delay D = 10 µs, and gate width W typically 300 µs). The signal is acquired between 503 to 715 nm (number of accumulation between 500 and 2000).

3 Results & Discussion

3.1 Radiation effects on solution composition and superplasticizer degradation products

The pH values, TOC, main inorganic and organic species measured in SP alkaline solutions and pore solutions extracted from non-irradiated (0 kGy) and irradiated (50, 100 and 250 kGy) grouts are summarized in Table S1 and Table S2 of the SI. The pH values are not changed after

irradiation for both types of solution. The TOC increase with dose in pore solutions, but this observation remains unexplained and would require more work.

To estimate the SPs degradation, the irradiated SP alkaline solutions were analyzed by IC (Table S1 of the SI). The measured concentration of sulfite and sulfate were summed-up, because sulfite anion were oxidized in sulfate with time. The markers of degradation from SP were identified in solution with acetate for PCE (Figure S1a of the SI) and with SO_3^{2-} and SO_4^{2-} for PNS (Figure S1b of the SI). The marker formation rate corresponding to the number of moles of markers formed by deposed energy in joules. This value is deduced of the slope of the line represented in Figure S1 of the SI. The markers formation rates are equivalent to (0.044 ± 0.008) and (0.017±0.002) µmol J^{-1} in PCE and PNS alkaline solutions, respectively. From each dose, an SP conversion rate (τ_{SP}) corresponding to the percentage of degraded polymer for a received dose was calculated using equation (4), in Table S3 of the SI. The marker and monomer mole are the number of moles of marker and monomer respectively, per kilogram of polymer.

$$\tau_{SP} = \frac{\text{marker mole}}{\text{monomer mole}} \times 100 \qquad (4)$$

In PCE and PNS alkaline solutions, the concentration of markers increases with the dose. The presence of sulfite and sulfate was measured without irradiation, only in PNS alkaline solution indicating that this SP was sensitive to alkaline hydrolysis degradation (Figure S1b of the SI). No acetate was measured without irradiation, so no hydrolysis of PCE is highlighted during this study, as noted in NDA (2015) (Figure S1a of the SI). The SPs structure seemed modified over 20% at 250 kGy after one year of hydrolysis (Table S3 of the SI). The modification can be induced by an alteration of SPs polymer chain, which can be combined with the loss of sulfonate groups for PNS. The SPs average molecular mass in weight ($\overline{M_w}$) were compared by

SEC in both SP alkaline solutions and pore solutions as a function of the dose in Figure 1 and Figure 2 for PCE and PNS, respectively.

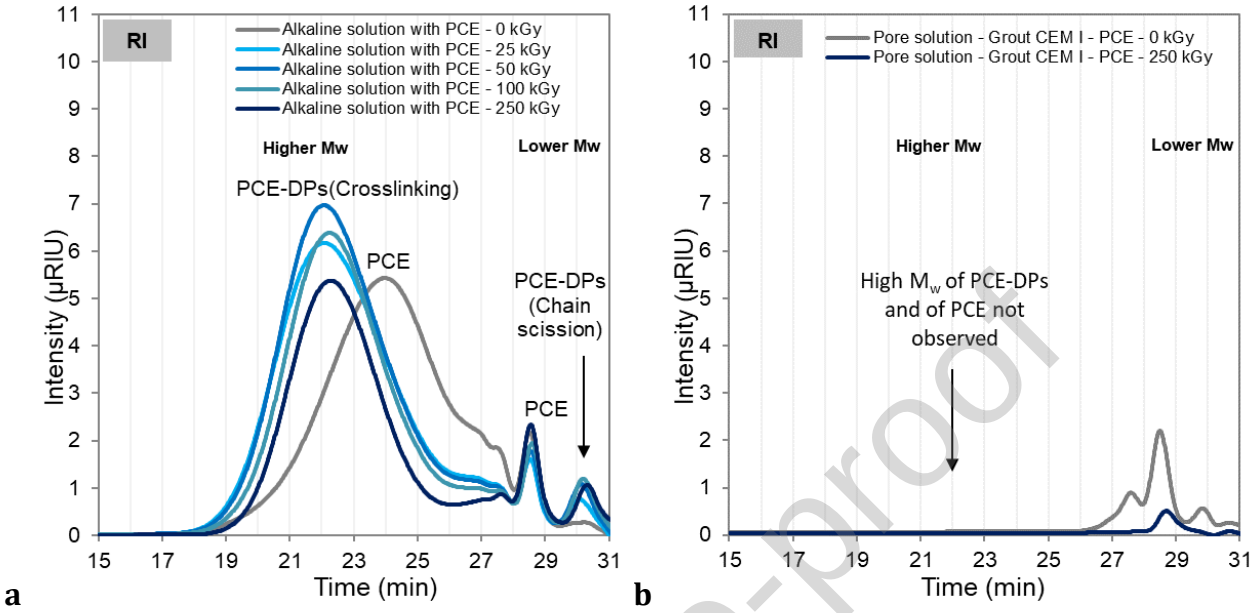

Figure 1. Size exclusion chromatograms of PCE alkaline solution as a function of the dose (from 0 to 250 kGy) (a), and of pore solution before (0 kGy) and after irradiation (250 kGy) (b) — Refractive Index detection.

The analysis of the non-irradiated PCE commercial solution revealed a broad peak at *ca*. 24 min corresponding to higher $\overline{M_w}$ as well as two peaks at 27.5 and 28.5 min with a lower intensity corresponding to lower $\overline{M_w}$. As expected, the three peaks are present in the non-irradiated alkaline solution with PCE (0 kGy, Figure 1a). After irradiation, whatever the dose, two changes were observed on Figure 1a. First, the main peak was shifted to a shorter retention time (22 min), which indicates an increase of $\overline{M_w}$ corresponding to a cross-linking phenomenon (García, 2018). Second, a new peak appeared at a longer retention time (30 min), which indicates decrease in $\overline{M_w}$ corresponding to a chain scission phenomenon (Baston et al., 2019). A radiolysis effect was observed on polymer structure from 25 kGy. The formation of DPs were observed in PCE alkaline solution whatever the dose. In pore solution, only PCE (27.5 and 28.5 min) and PCE-DPs (30 min) with molecules of low $\overline{M_w}$ were observed.

PCE (24 min) and PCE-DPs (cross-linking, 22 min) with molecules of high $\overline{M_w}$ were not detected (Figure 1b).

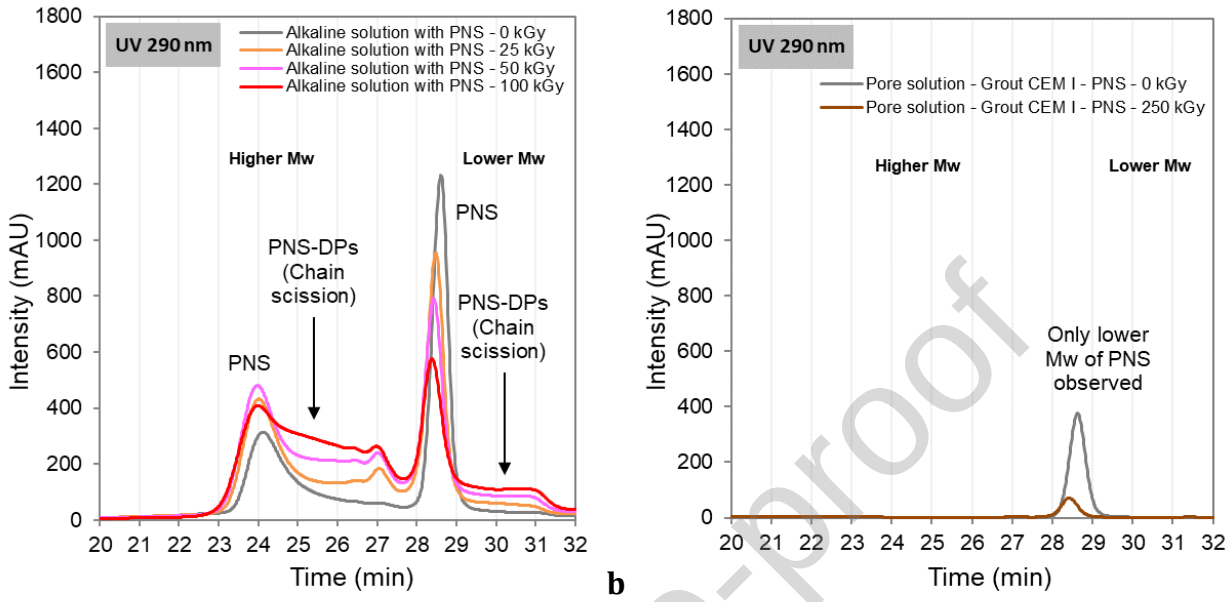

Figure 2. Size exclusion chromatograms of PNS alkaline solution as a function of the dose (from 0 to 100 kGy) (a), and of pore solution before (0 kGy) and after irradiation (250 kGy) (b) — UV detection at 290 nm.

The non-irradiated PNS commercial solution revealed two peaks corresponding to the highest (28.5 min) and lowest (24 min) molecular masses. As expected, they were present in the non-irradiated alkaline solution with PNS (0 kGy, (Figure 2a). After irradiation, whatever the dose, a tail is observed for each of these peaks on Figure 2a. This tail tends to increase with the dose. This phenomenon seems to indicate chain scissions of PNS initially present as a function of dose in alkaline solutions (Baston et al., 2019). The formation of DPs was observed in PNS alkaline solution as a function of dose. In pore solution (Figure 2b), only low $\overline{M_w}$ molecules of PNS polymer were observed (28.5 min), and neither PNS-DPs (tails) nor high $\overline{M_w}$ molecules of PNS (24 min) were detected.

3.2 Radiation effects on europium(III) solubility and aqueous speciation

3.2.1 *TRLFS*

As explained in § 2.2.7, TRLFS is based on the pulsed excitation of a fluorophore by a laser source. After excitation, the change in the Eu(III) fluorescence band ratio $^5D_0 \rightarrow {}^7F_2 / {}^5D_0 \rightarrow {}^7F_1$ is characteristic of complexed Eu species — see (Fromentin et al., 2020; Fromentin and Reiller, 2018; Reiller et al., 2017) and references therein. An increase of the band ratio of complexed Eu(III) species was observed in PCE alkaline solutions as a function of the dose (Figure 3a). In pore solutions, the formation of Eu-ligand complex was also observed (Figure 3b), but with a weaker intensity, after normalization at the TOC concentration (Table S1 and Table S2 of the SI). The ligands present in PCE alkaline solutions after hydrolysis and radiolysis seem to complex more Eu(III) than those present in pore solutions.

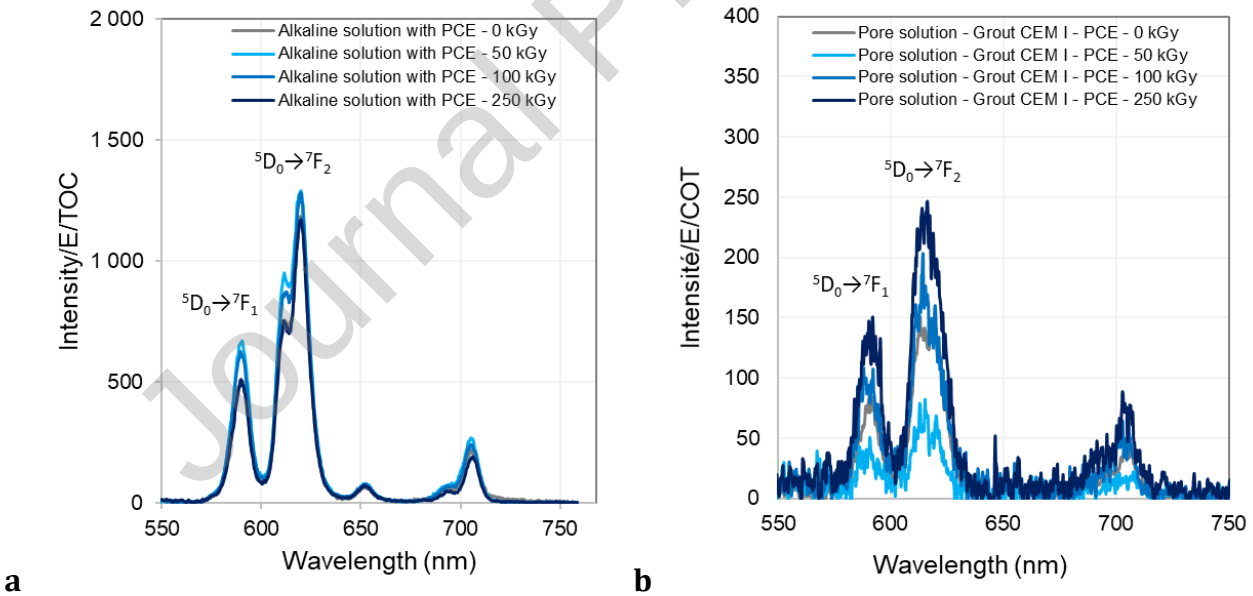

Figure 3. Evolution of luminescence spectra of Eu(III) in alkaline solutions (a) and in pore solutions (b) as a function of dose (from 0 to 250 kGy)— $[Eu]_{initial} = 10^{-6}$ mol L^{-1}; D = 10 µs, W = 300 µs, λ_{exc} = 393.8 nm.

During, the speciation of Eu-ligand in TRLFS, the luminescent properties of PNS masked the Eu signal so no conclusion could be made.

Unlike in previous works (Fromentin et al., 2020; Reiller et al., 2017), the degradation products were not available in a sufficient amount to allow interaction constants determination using TRLFS. Solubility experiments from oversaturated solutions were preferred to estimate the interaction coefficients.

3.2.2 *Solubility experiments*

Operational solubility experiments were performed on SP alkaline solutions as a function of the dose for PCE (Figure 4a) and PNS (Figure 5a). Similar experiments were done on SP alkaline solutions as a function of the dose after dilution in order to obtain a TOC content consistent with that measured in the pore solution: a 6-fold dilution for PCE (Figure 4b) and 10-fold dilution for PNS (Figure 5b). The TOC content was quantified in SPs alkaline solutions and in pore solutions as a function of the irradiation dose in Table S1 and Table S2 of the SI, respectively.

In alkaline solutions without SP, operational solubility results showed a dissolved Eu concentration of (2.1±0.7) 10^{-6} mol L^{-1} — i.e. $10^{-(5.7 \pm 1.9)}$ mol L^{-1} in Figure 4a —, close to the calculated dissolved Eu without SP — i.e. $10^{-(6.1 \pm 0.9)}$ mol L^{-1} shaded area in Figure 4a. In the presence of PCE, a significant increase of dissolved Eu was observed: *ca.* 30-fold higher for PCE (Figure 4a) and *ca.* 10-fold higher for PNS (Figure 5a), compared to the measure without SPs. This increase is the same at whatever dose for PCE (Figure 4b), but is proportional to the dose for PNS (Figure 5b) for the same TOC content. Even if the degradation products of cellulose are certainly different from those of SPs, Diesen et al. (2017) also observed an increase of europium(III) solubility in the presence of cellulosic degradation products. However, the operational Eu solubility in SP-grout pore solution is near the theoretically

dissolved Eu as a function of the dose for PCE (Figure 4c) and PNS (Figure 5c). There seems to be no significant impact of SP after the coupled effect of alkaline hydrolysis and radiolysis under these conditions.

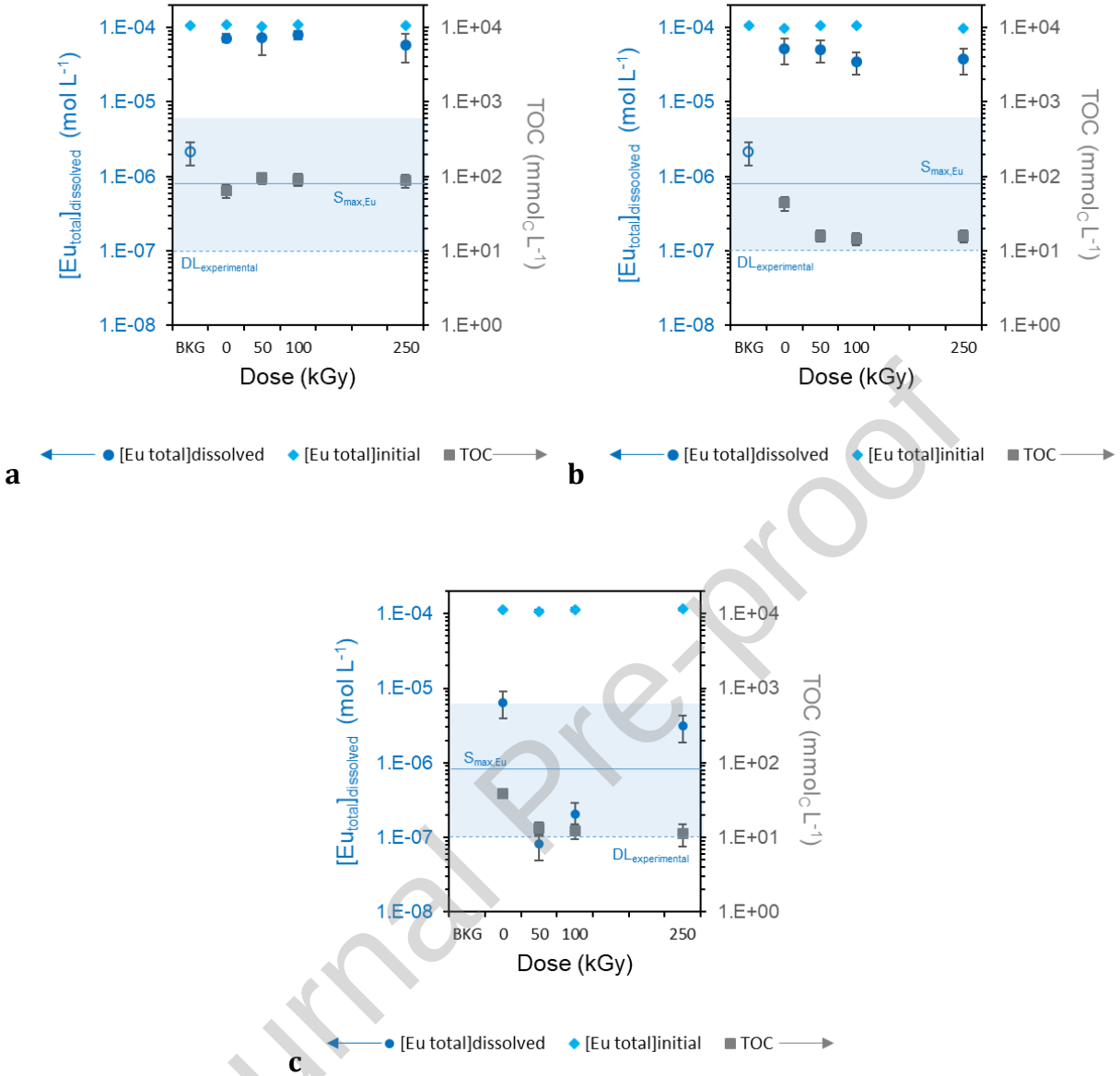

Figure 4. Concentration of total initial Eu (mol L^{-1}, blue diamonds), total dissolved Eu (mol L^{-1}, blue circles) and TOC content ($mmol_C$ L^{-1}, grey squares) in alkaline solution (without SP, BKG), in undiluted PCE alkaline solutions (a), in diluted PCE alkaline solutions (b) and in pore solutions (c) as a function of dose (from 0 to 250 kGy): Eu solubility limit in the medium $S_{max,Eu}$ (mol L^{-1}, blue plain line) with combined uncertainty (blue shaded area), Experimental detection limit DL_{exp} (mol L^{-1}, blue dotted line).

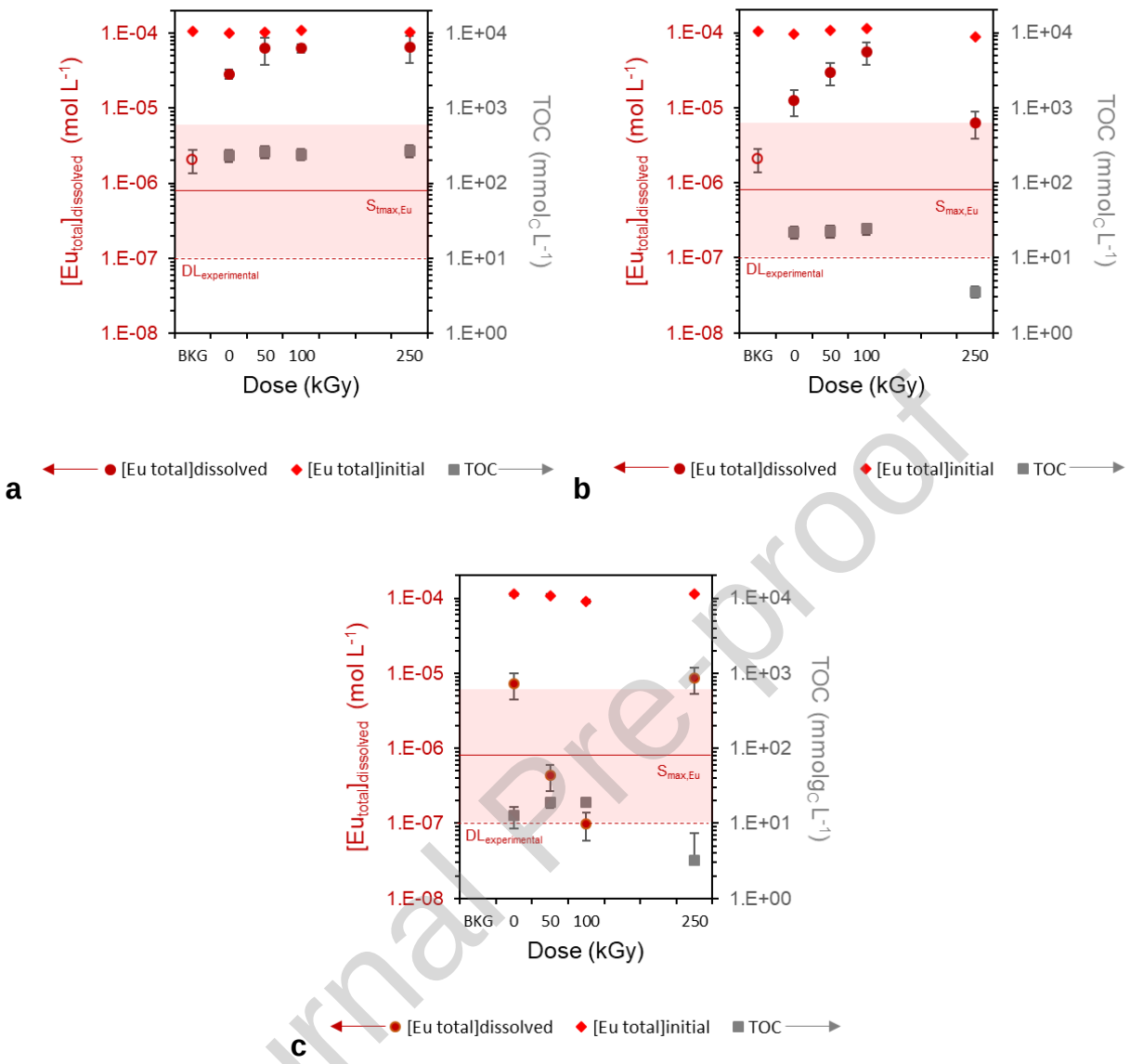

Figure 5. Concentration of total initial Eu (mol L^{-1}, red diamonds), total Eu dissolved (mol L^{-1}, red circles) and TOC content (mmol$_C$ L^{-1}, grey squares) in alkaline solution (without SP, BKG), in undiluted PNS alkaline solutions (a), in diluted PNS alkaline solutions (b) and in pore solutions as a function of dose (0 and 250 kGy) (c): Eu solubility limit in the medium $S_{max,Eu}$ (mol L^{-1}, plain red line) with combined uncertainty (red shaded area), experimental detection limit DL_{exp} (mol L^{-1}, red dotted line).

3.2.3 *Determination of operational interaction constants*

As the complete identification of the molecules and oligomers that compose the PCE- and PNS-DPs is not possible with the techniques used in this study, the functionality of DPs is unknown. Even if more complete studies were led (Chantreux, 2021; Chantreux et al., 2021; Isaacs et al., 2018), the identified molecules are not likely to complex Eu(III) under cementitious conditions. Furthermore, a substantial unidentified carbon pool still remains after the mass balance (Chantreux, 2021; Chantreux et al., 2021; Fromentin, 2017; Fromentin et al., 2017, 2016). Only operational complexation constants can be estimated based only on the amount of dissolved carbon, determined by TOC analysis, as already done elsewhere (Fromentin et al., 2020; Reiller et al., 2017).

The solubility constant K_s° of $Eu(OH)_3(am)$ is described as follows.

$$Eu(OH)_3(am) + 3H^+ \rightleftarrows Eu^{3+} + 3H_2O \qquad K_s^\circ = \frac{[Eu^{3+}]}{[H^+]^3} \tag{5}$$

with [i], the concentration of i (mol L^{-1})

The speciation of Eu(III) in the aqueous solution can be described by the side reaction coefficient $\alpha_{Eu^{3+}}$ (Ringböm, 1963) — see development in SI.

$$\alpha_{Eu^{3+}} = 1 + \sum_{n=1}^{3} \frac{{}^*\beta_n}{[H^+]^n} \tag{6}$$

with ${}^*\beta_n^\circ$ the standard state cumulative complexation constants of the hydrolysis equilibria.

$$Eu^{3+} + nH_2O \rightleftarrows Eu(OH)_n^{3-n} + H^+$$

$$ {}^*\beta_n^\circ = \frac{[Eu(OH)_n^{3-n}][H^+]^n}{[Eu^{3+}]} \tag{7}$$

Hence, the maximum solubility of Eu, $S_{max,Eu}$, depends on the solubility constants, pH, and the hydrolysis constants contained in side reaction coefficient,

$$K_s = \frac{S_{max,Eu}}{\alpha_{Eu^{3+}} [H^+]^3} \quad (8)$$

both for hydrolysis — mainly $Eu(OH)_3(aq)$ formation under these conditions as described extensively (Fromentin et al., 2020; Reiller et al., 2017) — and DPs complex formation based on the TOC value,

$$Eu^{3+} + hH_2O + lL \rightleftarrows Eu(OH)_hL_l + hH^+ \qquad K_{TOC} = \frac{[Eu(OH)_hL_l]\,[H^+]^h}{[Eu^{3+}][L]^l} \quad (9)$$

where the charges of both the ligand L and the complex are omitted for the sake of simplicity.

As it not possible to assign a charge to the complexing moieties, the ligands will be considered non-charged, so the charge of the free ion Eu^{3+} and of the complex (formally EuL^{3+}) will be the same and cancels out one another in the calculation of the ionic strength dependence.

The $\alpha_{Eu^{3+}}$ value can be extended and altered as follows:

$$\alpha_{Eu^{3+}} = 1 + \sum_{n=1}^{3} \frac{{}^*\beta_n}{[H^+]^n} + K_{TOC}\frac{[L]^l}{[H^+]^h} \cong \frac{{}^*\beta_3}{[H^+]^3} + K_{TOC}\frac{[L]^l}{[H^+]^h} \quad (10)$$

The $\log_{10}\ {}^*\beta_n$ value is linked to the standard conditions $\log_{10}\ {}^*\beta_n^\circ$ by the Davies (1962) equation for charged species. The activity coefficient of non-charged species L is linked to the Setchenow equation — see details in reference (Parkhurst and Appelo, 1999).

Contrary to previous studies (Fromentin et al., 2020; Reiller et al., 2017), neither the apparent stoichiometry *h* of H_2O nor the ligand higher than *l* = 1 can be ascertained due to the lack of solubility experimental points in equation (8).

Combining the inorganic solubility of $Eu(OH)_3(am)$ (equations 2 and 3) and the value of $\alpha_{Eu^{3+}}$ influenced by the organic DPs under these conditions (equation 10), a value of K_{TOC} with h = 0 and l = 1 can be proposed. The different $\log_{10}K_{TOC}$ values are reported in Figure 6, together with the averaged values and the standard deviations.

The $\log_{10}K_{TOC}$ values are little different whatever the doses and SPs. Only for PNS without dilution could the $\log_{10}K_{TOC}$ value be considered different from PCE and from PNS diluted. From the high complexation constant for $Eu(OH)_3(aq)$ (equation 2) in side reaction coefficient α (equation 10), the value of the product K_{TOC} [L] (with h = 0 and l = 1) is necessarily higher than ${}^{*}\beta_3/[H^+]^3$.

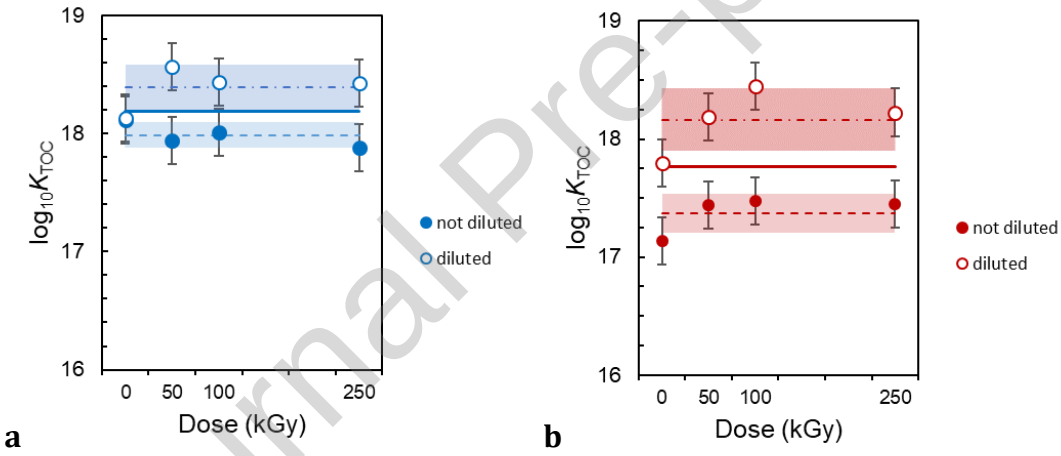

Figure 6. Logarithmic operational constants calculated from solubility experiment with PCE- DPs (Figure 4) and PNS-DPs (b) (Figure 5), either undiluted (filled circles) or diluted (open circles), in alkaline solutions as a function of the dose : averaged values are in dashed (undiluted), dot-dashed (diluted), and plain (grand averaged) lines; shaded areas represent the standard deviations of the averaged values.

Using $\log_{10}K_{TOC}$ from Figure 6, the calculated solubility of $Eu(OH)_3(am)$ *vs.* TOC concentration (Figure 7) is not changed up to 10^{-4} mol_C L^{-1} independently of the SP. Considering the uncertainties, the values cannot be considered significantly different. It requires *ca.* 10^{-2} mol_C L^{-1} to observe a one order of magnitude increase in Eu(III) solubility. It is also interesting

to compare the influence of these $\log_{10}K_{TOC}$ on $Eu(OH)_3(am)$ solubility with the equivalent ones determined for polyvinyl chloride (PVC) and polyester urethane (PUR) radiolysis DPs under the same pH conditions — see *e.g.* $Eu(OH)_2L_3$ in Table S2 of the SI from Reiller et al. (2017) and EuL at pH 13.3 in Table S3 of the SI from Fromentin et al. (2020). It seems though that the DPs from SPs show slightly more important complexation properties compared to both PVC and PUR radiolysis DPs, based on the TOC quantity (Figure 7). Comparing our results with previously published results (Fromentin et al., 2020; Reiller et al., 2017), a concentration of 0.1 $mol_C\ L^{-1}$ of SP-DPs induces a higher solubility of $Eu(OH)_3(am)$ than a concentration of 1 $mol_c\ L^{-1}$ of PVC-DPs — see dot-dashed line in Figure 7 — or PUR-DPs — see double dot-dashed line in Figure 7.

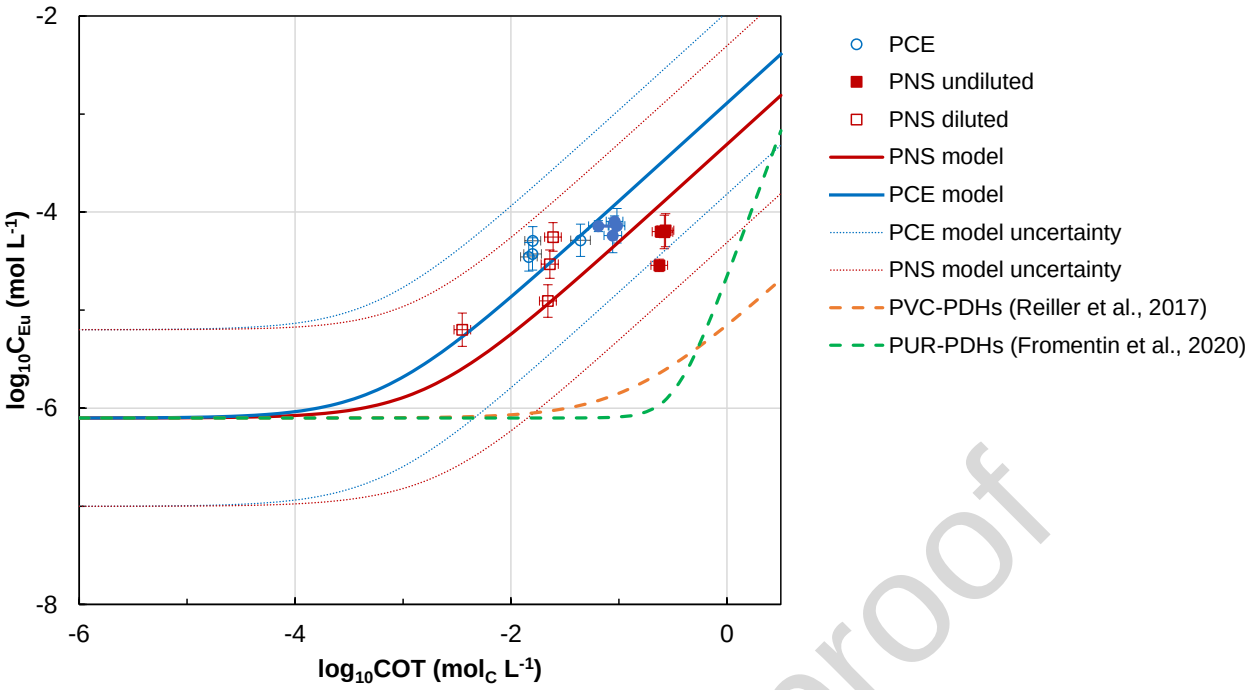

Figure 7. Calculated Eu(III) solubility under experimental conditions of Figure 4 (PCE, blue circles) and Figure 5 (PNS, red squares), for undiluted (filled symbols) and diluted (open symbols), using grand averaged $\log_{10}K_{TOC}$ values for PCE (plain blue line) and PNS (dashed red line): the error bars represent 2σ values of concentration determinations, and the dotted lines represent the standard deviation of solubility, calculated by propagation of errors; the green dot-dashed line represents the solubility considering PVC-DP complex $Eu(OH)_2L_3$ (Reiller et al., 2017); the orange double dot-dashed line represents solubility considering PUR-DP complex EuL determined at pH 13.3 (Fromentin et al., 2020).

3.2.4 *Rationale of complexation of Eu(III) by DPs, and consequences on Eu(III) solubility in SP based cement*

It has been shown that whatever the dose, the Eu solubility remains unchanged with PCE-DPs in alkaline solutions. Conversely, the PNS seems to increase the Eu solubility with the content of associated degradation products in alkaline solutions. The latter increase helps to explain the increase of Eu solubility with the dose in alkaline solutions. Organic compounds present in

pore solution are different from those in SP alkaline solution. High $\overline{M_w}$ molecules of SP and SP-DPs were not observed in pore solution. Only a small quantity of low $\overline{M_w}$ molecules of SP and/or SP-DPs was observed in pore solution and did not have any effect on the Eu solubility in pore solution. Only high $\overline{M_w}$ molecules of SP seem to increase Eu solubility, but they do not seem to be released in pore solution.

SEC experiments have shown modifications of $\overline{M_w}$ from SPs in alkaline solution after irradiation (crosslinking and/or chain scission). This modification revealed a significant conversion rate but SP degradation products and high $\overline{M_w}$ molecules were not detected in pore solution. This observation may help to explain the difference of operational solubility in SP alkaline and pore solutions for the same TOC concentration. A limited effect of the coupled effect of radiolysis and alkaline hydrolysis of SP on Eu solubility in pore solution was observed.

The Eu solubility was increased with alkaline DPs of both SPs, but as the DPs present in pore solution were not the same as in alkaline solution, the impact on Eu solubility in pore water seems relatively minimal. Two phenomena could be proposed: (i) the competition with dissolved metals in the pore solution, i.e. Ca, Al, and Fe; and (ii) the adsorption of DPs at the surface of cementitious minerals or incorporation in the structure of composing phases as observed for other organic ligands (Pointeau et al., 2008, 2006; Pöllmann et al., 2006) leaving DPs that have lower affinities for Eu in the pore solution.

The first hypothesis can be tested through a theoretical exercise on the solubility of $Eu(OH)_3(am)$ in the presence of CSH1.6 ($Ca_{1.6}SiO_{3.6}$:$2.58H_2O$) phase (Blanc et al., 2010) as a simplified mineralogical assemblage of cementitious phases, or Ca buffer — the actual assemblage should be composed of e.g. jennite, portlandite, ettringite, hydrogarnet, hydrotalcite, Na_2O and K_2O —, using PHREEQC and varying the interaction constant of a

possible Ca-DP complex equivalent to equation (10) with h = 0 and l = 1, and using the interaction constants for Eu-PCE and -PNS determined in the previous section. First, Figure S2a of the SI reflects that a higher $\log_{10}K_{TOC}$ is needed for PNS compared to PCE to obtain the same $S_{max,Eu}$ value. Second, a $\log_{10}K_{Ca\text{-}DP}$ *ca.* 5.5 would be necessary to decrease the $S_{max,Eu}$ value of one (PCE) or half an order of magnitude, and *ca.* 7 to impede the solubility increase completely. It would also induce an increase in $S_{max,Ca}$ in the pore solution (Figure S2b), which is not observed in Table S2 of the SI compared to equilibrium solution at the same pH value (Pointeau et al., 2006). With these calculation the adsorption at the surface and/or incorporation in the structure of the cementitious phases seem more likely.

4 Conclusions

In the context of intermediate-level long-lived cemented nuclear waste, the degradation phenomena of superplasticisers (polycarboxylate ether and polynaphtalene sulfonate) were studied under inert conditions: under basic hydrolysis, and by coupling alkaline hydrolysis and radiolysis. Alkaline hydrolysis occurred at pH higher than 12.5. Radiolysis was achieved under γ-irradiation with a dose rate of 1 kGy h^{-1} and doses between 0 and 250 kGy. Two types of equilibrium solution were degraded: i) irradiated SP alkaline solutions containing a concentration of SP in solution more appropriate to characterize DPs, and ii) pore solutions obtained by pressing irradiated SP-grout, to approach real conditions. Eu(III) was used to simulate the solubility of a +III redox state radionuclide. Our main objective was to understand, during interactions with Eu(III), the impact of DPs resulting from the coupled effect of alkaline hydrolysis and radiolysis of superplasticisers.

In alkaline solutions, modifications of the average molecular weight of SPs were shown for two superplasticisers — crosslinking and chain scissions phenomena were observed as a function of the dose, after irradiation. These modifications have suggested significant polymer

conversion rates of 22-25% at 250 kGy A difference of solubility between superplasticisers in alkaline and pore solutions was measured for the same total organic carbon concentrations. The small quantity of low $\overline{M_w}$ molecules leached in pore solution have a weak interaction with Eu(III), which can explain the difference of operational solubility between superplasticisers alkaline and pore solutions. A change in the complexation of Eu(III) was confirmed by time-resolved laser-induced fluorescence spectroscopy investigations in polycarboxylate ether in alkaline solutions, and suggested in pore solutions, but the signal is much lower in pore solutions.

The effects obtained by adding superplasticiser to an alkaline solution are not representative of those observed in interstitial solution, and that solubility of actinides(III) in radiolyzed admixed cement would not be influenced by the formation of degradation product of superplasticisers. In this study, no significant impact of coupled effect of radiolysis for doses lower than 250 kGy, and alkaline hydrolysis (pH 12.9) of SPs on Eu(III) solubility in pore solution (SP-grout with 1 and 2wt% of PCE and PNS, respectively) were observed.

Environmental implication

Superplasticizers are used as admixtures to increase the workability of the early-age cement-water-aggregate mixture. In a nuclear deep geological disposal situation, SP undergo coupled effect of radiolysis and hydrolysis in near the pore solution of cementbased materials. Determining the impact of SP degradation products on radionuclides transfer through cementitious materials is important for assessing the disposal concept. For that, this work focalized the study of pore solutions obtained by pressing SP-grout irradiated, as reference to an SP cement-based compact system.

CRediT authorship contribution statement

Solène Legand: Investigation, Methodology, Data Curation, Writing – Original Draft, Writing – Review and Editing, Visualization, Validation **Nathalie Macé**: Conceptualization, Validation, Resources, Supervision **Benoist Muzeau**: Conceptualization, Validation, Resources, Supervision **Philippe Le Tutour**: Methodology, Investigation **Sandrine Therias**: Supervision,

Writing – Review and Editing **Pascal E. Reiller**: Supervision, Writing – Original Draft, Writing – Review and Editing, Conceptualization, Formal Analysis, Visualization

Declaration of Competing Interest

The authors declare the following financial interests/personal relationships which may be considered as potential competing interests: LEGAND Solene (CEA) reports financial support was provided by French National Agency for Radioactive Waste Management (ANDRA). LEGAND Solene (CEA) reports financial support was provided by French Alternative Energies and Atomic Energy Commission (CEA). LEGAND Solene (CEA) reports financial support was provided by EDF. LEGAND Solene (CEA) reports financial support was provided by Orano.

Acknowledgements

The authors acknowledge Andra, EDF, and Orano for their financial support and scientific exchanges; F. Carpentier, S. Esnouf, and J. Page for their contributions to this study; and the anonymous reviewers for their suggestions.

References

Andra, 2005. Dossier 2005. Argile. Tome Evolution phénoménologique du stockage géologique. p. 520. ANDRA, http://www.andra.fr/sites/default/files/2018-02/269.pdf.

Baston, G., Dawson, J., Farahani, B., Saunders, R., Schofield, J., Smith, V., 2019. Further studies to underpin the use of PCE superplasticisers in the packaging of low-heat-generating wastes. Updates on the effects of radiolysis products on sorption and solubility (Contractor Report to RWM No. NDA Report no. RWM/Contr/19/035). https://rwm.nda.gov.uk/publication/further-studies-to-underpin-the-use-of-pce-superplasticisers-in-the-packaging-of-low-heat-generating-wastes/.

Binnemans, K., 2015. Interpretation of europium(III) spectra. Coord. Chem. Rev. 295, 1–45. https://doi.org/10.1016/j.ccr.2015.02.015

Blanc, Ph., Bourbon, X., Lassin, A., Gaucher, E.C., 2010. Chemical model for cement-based materials: Temperature dependence of thermodynamic functions for nanocrystalline and crystalline C–S–H phases. Cem. Concr. Res. 40, 851–866. https://doi.org/10.1016/j.cemconres.2009.12.004

Carnall, W.T., Fields, P.R., Rajnak, K., 1968. Electronic energy levels of the trivalent lanthanide aquo ions. IV. Eu^{3+}. Chem. Phys. 49, 4450–4455. https://doi.org/10.1063/1.1669896

Chantreux, M., 2021. Etude de la dégradation par radiolyse et/ou hydrolyse basique de PVC présents dans les stockages de déchets radioactifs (These de doctorat). Aix-Marseille. https://www.theses.fr/2021AIXM0517.

Chantreux, M., Ricard, D., Asia, L., Rossignol, S., Wong-Wah-Chung, P., 2021. Additives as a major source of radiolytic organic byproducts of polyvinyl chloride (PVC). Radiat. Phys. Chem. 188, 109671. https://doi.org/10.1016/j.radphyschem.2021.109671

Chernyshev, A., Jonsson, M., Forsberg, K., 2018. Characterization and degradation of a polyaryl ether based superplasticizer for use in concrete barriers in deep geological repositories. Appl. Geochem. 95, 172–181. https://doi.org/10.1016/j.apgeochem.2018.05.014

Chernyshev, A.N., Maier, A.C., Jonsson, M., Forsberg, K., 2021. Solubilisation of Ni(II) and Eu(III) through complexation with a polyaryl ether based superplasticizer in alkaline media. Chemosphere 263, 127686. https://doi.org/10.1016/j.chemosphere.2020.127686

Clacher, A., Marshall, T., Swanton, S., 2013. Solubility studies : effect of ADVA cast 551 at low concentration. Amec report 004249/001 Issue 04, p.50. https://rwm.nda.gov.uk/publication/amec_ts_004249_001-issue-04/

Cyr, M., Daidié, A., 2007. Optimization of a high-pressure pore water extraction device. Rev. Sci. Instrum. 78, 023906. https://doi.org/10.1063/1.2428273

Cyr, M., Rivard, P., Labrecque, F., Daidié, A., 2008. High-Pressure Device for Fluid Extraction from Porous Materials: Application to Cement-Based Materials. J. Am. Ceram. Soc. 91, 2653–2658. https://doi.org/10.1111/j.1551-2916.2008.02525.x

Davies, C.W., 1962. Ion association. Butterworths, London, UK.

Diesen, V., Forsberg, K., Jonsson, M., 2017. Effects of cellulose degradation products on the mobility of Eu(III) in repositories for low and intermediate level radioactive waste. J. Hazard. Mater. 340, 384–389. https://doi.org/10.1016/j.jhazmat.2017.07.008

Dobbs, J.C., Susetyo, W., Carreira, L.A., Azarraga, L.V., 1989. Competitive binding of protons and metal ions in humic substances by lanthanide ion probe spectroscopy. Anal. Chem. 61, 1519–1524. https://doi.org/10.1021/ac00189a012

Felekoğlu, B., Sarıkahya, H., 2008. Effect of chemical structure of polycarboxylate-based superplasticizers on workability retention of self-compacting concrete. Constr. Build. Mater. 22, 1972–1980. https://doi.org/10.1016/j.conbuildmat.2007.07.005

Flatt, R., Schober, I., 2012. Superplasticizers and the rheology of concrete, in: Roussel, N. (Ed.), Understanding the Rheology of Concrete, Woodhead Publishing Series in Civil and Structural Engineering. Woodhead Publishing, pp. 144–208. https://doi.org/10.1533/9780857095282.2.144

Fröhlich, D.R., Koke, C., Maiwald, M.M., Chomyn, C., Plank, J., Panak, P.J., 2019. A spectroscopic study of the complexation reaction of trivalent lanthanides with a synthetic acrylate based PCE-superplasticizer. Spectrochim. Acta A 207, 270–275. https://doi.org/10.1016/j.saa.2018.09.025

Fröhlich, D.R., Maiwald, M.M., Taube, F., Plank, J., Panak, P.J., 2017. A thermodynamical and structural study on the complexation of trivalent lanthanides with a polycarboxylate based concrete superplasticizer. Dalton Trans. 46, 4093–4100. https://doi.org/10.1039/C7DT00200A

Fromentin, E., 2017. Lixiviation des polymères irradiés : caractérisation de la solution et complexation des actinides (thesis). Université Pierre et Marie Curie - Paris VI. https://tel.archives-ouvertes.fr/tel-01622137v1.

Fromentin, E., aymes-chodur, C., Doizi, D., Cornaton, M., Miserque, F., Cochin, F., Ferry, M., 2017. On the radio-oxidation, at high doses, of an industrial polyesterurethane and its pure resin. Polym. Degrad. Stab. 146. https://doi.org/10.1016/j.polymdegradstab.2017.10.007

Fromentin, E., Lebeau, D., Bergounioux, A., Ferry, M., Reiller, P.E., 2020. Interactions between hydro-soluble degradation products from a radio-oxidized polyesterurethane and Eu(III) in contexts of repositories for low and intermediate level radioactive waste. Radiochim. Acta 108, 383–385. https://doi.org/10.1515/ract-2019-3122

Fromentin, E., Pielawski, M., Lebeau, D., Esnouf, S., Cochin, F., Legand, S., Ferry, M., 2016. Leaching of radio-oxidized poly(ester urethane): Water-soluble molecules characterization. Polym. Degrad. Stab. 128, 172–181. https://doi.org/10.1016/j.polymdegradstab.2016.03.007

Fromentin, E., Reiller, P.E., 2018. Influence of adipic acid on the speciation of Eu(III): review of thermodynamic data in NaCl and $NaClO_4$ media, and a new determination of Eu-adipate complexation constant in 0.5mol.kg_w^{-1} $NaClO_4$ medium by time-resolved luminescence spectroscopy. Inorg. Chim. Acta 482, 588–596. https://doi.org/10.1016/j.ica.2018.06.035

García, D.M., 2018. The role of superplasticizers and their degradation products on radionuclide mobility (thesis). Universitat Politècnica de Catalunya. https://upcommons.upc.edu/bitstream/handle/2117/122700/TDMGC1de1.pdf?sequence=1&isAllowed=y, Barcelona.

Greenfield, B.F., Ilett, D.J., Ito, M., McCrohon, R., Heath, T.G., Tweed, C.J., Williams, S.J., Yui, M., 1998. The effect of cement additives on radionuclide solubilities. Radiochim. Acta 82, 27–32. https://doi.org/10.1524/ract.1998.82.special-issue.27

Guérandel, C., Vernex-Loset, L., Krier, G., De Lanève, M., Guillot, X., Pierre, C., Muller, J.F., 2011. A new method to analyze copolymer based superplasticizer traces in cement leachates. Talanta 84, 133–140. https://doi.org/10.1016/j.talanta.2010.12.022

Horrocks, W.D., Sudnick, D.R., 1979. Lanthanide ion probes of structure in biology. Laser-induced luminescence decay constants provide a direct measure of the number of metal-coordinated water molecules. J. Am. Chem. Soc. 101, 334–340. https://doi.org/10.1021/ja00496a010

Hummel, W., Berner, U., Curti, E., Pearson, F.J., Thoenen, T., 2002. Nagra/psi chemical thermodynamic data base 01/01 (No. Technical report 02-16. NAGRA, Wettingen, Switzerland). https://www.dora.lib4ri.ch/psi/islandora/object/psi:11583.

Isaacs, M., Hinchliff, J., Felipe-Sotelo, M., Read, D., 2018. Factors affecting the suitability of superplasticiser-amended cement for the encapsulation of radioactive waste. Advances in Cement Research 30, 216–230. https://doi.org/10.1680/jadcr.17.00099

Kitamura, A., Fujiwara, K., Mihara, M., Cowper, M., Kamei, G., 2013. Thorium and americium solubilities in cement pore water containing superplasticiser compared with thermodynamic calculations. J. Radioanal. Nucl. Chem. 298, 485–493. https://doi.org/10.1007/s10967-013-2618-4

Lezane, A., 1994. Incidence des adjuvants pour béton sur le confinement des radioéléments et la tenue sous rayonnement des matrices “ciments” (thesis). Université René Descartes - Paris V, Paris, France. https://inis.iaea.org/collection/NCLCollectionStore/_Public/47/096/47096912.pdf.

NDA, 2015. Solubility studies in the presence of polycarboxylate ether superplasticisers DA DRP LOT 2: Integrated Waste Management WP/B2/7 Ref. S2885/500/003, p.121.

https://assets.publishing.service.gov.uk/government/uploads/system/uploads/attachment_data/file/476842/Solubility_Studies_in_the_Presence_of_Polycarboxylate_Ether_Superplasticisers_-_August_2015.pdf

Palacios, M., Puertas, F., 2004. Stability of superplasticizer and shrinkage-reducing admixtures in high basic media. Mat. de Construccion 54, 65–86. https://doi.org/10.3989/mc.2004.v54.i276.256

Parkhurst, D.L., Appelo, C.A.J., 1999. User's guide to PHREEQC (version 2) a computer program for speciation, batch-reaction, one-dimensional transport, and inverse geochemical calculations (Rapport U.S. Geological Survey No. Water-Resources Investigations, 99-4259). Lakewood, Colorado (U.S.A) https://doi.org/10.3133/wri994259.

Pointeau, I., Coreau, N., Reiller, P.E., 2008. Uptake of anionic radionuclides onto degraded cement pastes and competing effect of organic ligands. Radiochim. Acta 96, 367–374. https://doi.org/10.1524/ract.2008.1503

Pointeau, I., Hainos, D., Coreau, N., Reiller, P.E., 2006. Effect of organics on selenite uptake by cementitious materials. Waste Manage., Mechanisms and Modeling of Waste/Cement Interactions 26, 733–740. https://doi.org/10.1016/j.wasman.2006.01.026

Pöllmann, H., Stefan, S., Stern, E., 2006. Synthesis, characterization and reaction behaviour of lamellar AFm phases with aliphatic sulfonate-anions. Cem. Concr. Res. 36, 2039–2048. https://doi.org/10.1016/j.cemconres.2006.06.008

Reiller, P.E., Fromentin, E., Ferry, M., Dannoux-Papin, A., Badji, H., Tabarant, M., Vercouter, T., 2017. Complexing power of hydro-soluble degradation products from γirradiated polyvinylchloride: influence on $Eu(OH)_3(s)$ solubility and Eu(III) speciation in neutral to alkaline environment. Radiochim. Acta 105, 665–675. https://doi.org/10.1515/ract-2016-2691

Ringböm, A., 1963. Complexation in analytical chemistry: a guide for the critical selection of analytical methods based on complexation reactions., Chemical analysis. Interscience Publishers, New York, NY, USA. https://searchworks.stanford.edu/view/4735949.

Thoenen, T., Hummel, W., Berner, U., Curti, E., 2014. The PSI/Nagra chemical thermodynamic database 12/07 (No. Report PSI Bericht Nr 14-04 (ISSN 1019-0643). Paul Scherrer Institute, Villigen, Switzerland). https://www.psi.ch/sites/default/files/import/les/DatabaseEN/PSI-Bericht%252014-04_final_druckerei.pdf.

Von Sonntag, C., 2003. Free-radical-induced chain scission and cross-linking of polymers in aqueous solution—an overview. Radiat. Phys. Chem., 10th Tihany Symposium on Radiation Chemistry 67, 353–359. https://doi.org/10.1016/S0969-806X(03)00066-5

Yilmaz, V.T., Odabaoğlu, M., Içbudak, H., Ölmez, H., 1993. The degradation of cement superplasticizers in a high alkaline solution. Cem. Concr. Res. 23, 152–156. https://doi.org/10.1016/0008-8846(93)90146-Z

Zini, Q., Buldini, P.L., Morettini, L., 1985. Rapid determination of dissolved silica in natural waters. Microchemical Journal 32, 148–152. https://doi.org/10.1016/0026-265X(85)90070-0

Graphical abstract

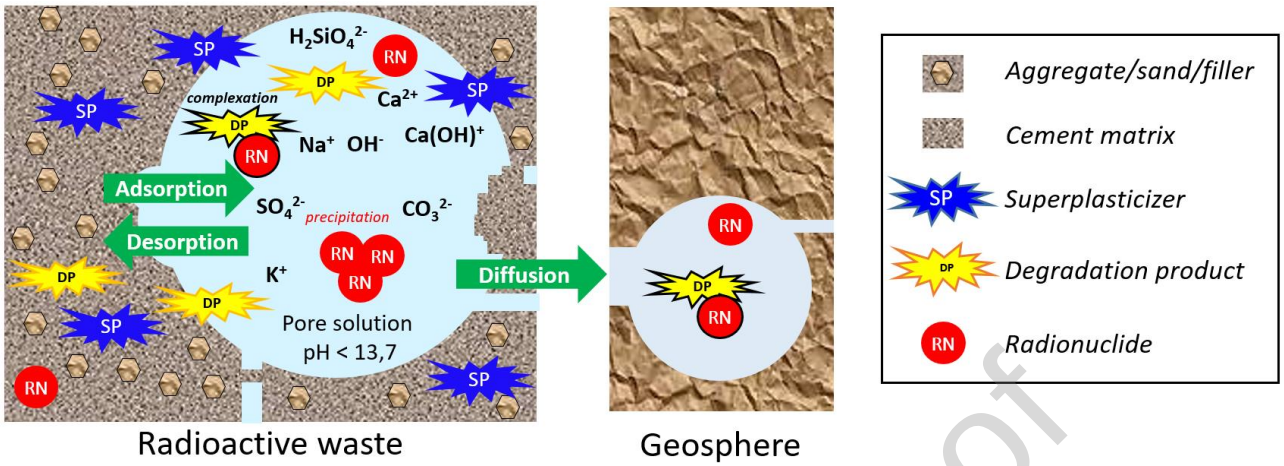

Highlights

- Solubility results in artificial cement water are not representative of those obtained in interstitial water.
- Solubility results are obtained in interstitial solutions from irradiated admixed cementitious materials.
- Solubility results for show comparable results for two commercial superlasticiser solutions (with additives).